

# Morphology study of rubber based nanocomposites by transmission electron microscopy and atomic force microscopy

S. SADHU, A. K. BHOWMICK\*

Rubber Technology Centre, Indian Institute of Technology, Kharagpur 721302, India  
E-mail: anilkb@rtc.iitkgp.ernet.in

Rubber based nanocomposites were prepared using octadecyl amine modified Na-montmorillonite clay (OC) and Styrene Butadiene Rubber (SBR) having styrene content of 15, 23 and 40% respectively and Acrylonitrile Butadiene Rubber (NBR) having acrylonitrile content of 19, 34 and 50% respectively. The morphology of the nanocomposites was investigated using Atomic Force Microscopy (AFM), Transmission Electron Microscopy (TEM) and X-ray Diffraction Technique (XRD). The TEM photographs of the unmodified clay loaded SBR nanocomposite showed agglomeration, while the modified clay loaded SBRs of all the grades revealed complete exfoliation. The NBRs, on the other hand, gave unexfoliated and intercalated clay structures both with the unmodified and the modified clays, except in the case of NBR having 19% of acrylonitrile and 4% of the unmodified clay. The AFM data were in good accord with the TEM results. The particle dimensions were within the range of 10–20 nm in the case of SBR sample having 4 parts of the modified clay. NBRs having 34 and 50% acrylonitrile contents and 4 parts of OC showed clay particles ranging from 50–70 nm and 70–100 nm respectively. On comparison of the rubbers having different nature and contents of functional groups and filler loadings, significant effect on the morphology of the composite was observed. The nature of solvent used to prepare the nanocomposites also affected the morphology. XRD data further corroborated the facts in all the above cases. © 2005 Springer Science + Business Media, Inc.

## 1. Introduction

The addition of active fillers into elastomers is of significant commercial importance, due to the improvement of various technical properties of the final materials. Clays have long been used as fillers in polymeric systems because of low cost and the improved mechanical properties of the resulting composite. The efficiency of a filler to improve physico-mechanical properties of the polymer system is sensitive to the degree of dispersion in the polymer matrix [1]. Until recently clays could be dispersed on a microscale only. Toyota researchers [2] discovered that the treatment of montmorillonite clay with aminoacids allows dispersion of the individual 1 nm thick silicate layers of the clay on a nanometer scale in polyamide 6. Their hybrid materials have shown major improvements in physical and mechanical properties even at very low clay content (1.6 vol%). Numerous other researchers used this concept later on for preparation of nanocomposites based on epoxies [3–5], unsaturated polyester [6], poly ( $\epsilon$ -caprolactone) [7], poly (ethylene oxide) [8], silicone rubber [9, 10], polystyrene [11], polyimide [12], polypropylene [13],

poly (ethylene terephthalate) [14] and polyurethane [15]. We have also reported preparation and properties of nanocomposites based on several rubbers like, acrylonitrile butadiene rubber (NBR), styrene butadiene rubber (SBR) and polybutadiene rubber (BR) [16].

Nanoscale layered clays with very high aspect ratio and high strength can play an important role in forming effective nanocomposites owing to their intercalation chemistry. The level or extent of dispersion depends on the nature of matrix, the plasticizer or coupling agent and the level of interaction between the clay and the matrix. When the nanoparticles are dispersed in a polymer matrix, two types of nanocomposites can be obtained. Intercalated nanocomposites are formed when there is limited inclusion of polymer chain between the clay layers, with a small increase in the interlayer spacing of a few nanometers. On the other hand, exfoliated structures are formed when the clay layers are well separated from one another and individually dispersed in the polymer matrix. Until recently, the dispersion of fillers has been determined predominantly by

\*Author to whom all correspondence should be addressed.

optical and transmission electron microscopy (TEM) [17, 18]. However, electron microscopy requires the painful preparation of microtome sections. Now a days Atomic Force Microscopy (AFM) is also a very good tool which gives an insight into surface morphology of composites. This technique is finding applications in rubber science only recently [19, 20]. X-ray Diffraction Technique (XRD) has been used extensively to calculate the gallery gap from the  $2\theta$  values to understand the extent of intercalation. Exfoliated nanocomposites do not show any peak due to absence of any layered structure.

In this paper, Atomic Force Microscopy (AFM) and Transmission Electron Microscopy (TEM) are used as effective tool for qualitative and quantitative analysis of dispersion of nanoclay in nitrile rubber (NBR) and styrene-butadiene rubber (SBR) nanocomposites and to understand the influence of nature of clay and copolymer composition and polarity of the rubber on the intercalation and exfoliation processes. XRD data are used for correlation.

## 2. Experimental

### 2.1. Materials

Styrene-butadiene rubber (SBR) (Synaprene -1502) having Mooney Viscosity  $M_L$  (1+4) at 100°C = 52 and styrene content 23% was supplied by Synthetics and Chemicals Ltd., Bareilly, India. Other styrene butadiene rubbers having 15% (Mooney Viscosity,  $M_L$  (1+4) at 100°C = 131) and 40% (Mooney Viscosity,  $M_L$  (1+4) at 100°C = 75) styrene contents were supplied by Apcotex Lattices Ltd., Mumbai, India. Two grades of nitrile rubber (NBR) with different acrylonitrile contents [19% { $M_L$  (1+4) at 100°C = 60} and 50% { $M_L$  (1+4) at 100°C = 58}] were supplied by Bayer Ltd, Canada. NBR with 34% nitrile content [ $M_L$  (1+4) at 100°C = 43] was supplied by APAR, Mumbai, India. Toluene and chloroform were procured from MERCK (India) Ltd., Mumbai and RANBAXY (India) Ltd. S.A.S Nagar respectively; Na<sup>+</sup>-montmorillonite was generously supplied by Southern Clay Products, USA. The stearyl amine was obtained from SIGMA CHEMICAL CO. Mumbai, India. Dicumyl peroxide produced by Hercules Inc., USA was used as the crosslinking agent for the rubbers. Ethyl alcohol was supplied by Bengal Chemicals and Pharmaceuticals, Kolkata, India.

### 2.2. Preparation of nanoclays

5 gms of the clay was dispersed in 400 cc water at 80°C for half an hour. 2 gms of octadecyl amine was added with concentrated HCl (5 cc) and the resulting octadecyl ammonium chloride was dissolved in 200 cc hot water. This solution was then added to the clay dispersion at 80°C with constant stirring slowly. Then the modified clay was filtered, washed several times to make sure that it was free of chloride ions (as tested by silver nitrate solution) and dried it at room temperature (30°C) in vacuum. Their designations are given in Table I.

TABLE I Materials and abbreviations

Material	Abbreviations
Unmodified Na-montmorillonite	N
Modified montmorillonite	OC
Styrene butadiene rubber with 15% styrene content	15SBR
Styrene butadiene rubber with 23% styrene content	23SBR
Styrene butadiene rubber with 40% styrene content	40SBR
Acrylonitrile Butadiene Rubber with 19% acrylonitrile content	19NBR
Acrylonitrile Butadiene Rubber with 34% acrylonitrile content	34NBR
Acrylonitrile Butadiene Rubber with 50% acrylonitrile content	50NBR

### 2.3. Preparation of clay-rubber nanocomposite

The rubber was first dissolved in a solvent—toluene for SBR and chloroform for NBR. The modified clay was dispersed in ethyl alcohol. The required amount of clay dispersion was poured into the rubber solution and the mixture was agitated for 2 h. Dicumyl Peroxide was also added to this solution during stirring (1 phr) as a curing agent. This solution was then dried in a vacuum oven at 50°C for 2 days to drive out the solvents. The samples were then passed through open two-roll mill and then molded at 160°C for the optimum cure time, obtained from a rheometer MDR-2000, to prepare sheets of 1 mm thickness. The designation and a list of the nanocomposites prepared is given in Tables I and II. The samples are designated as ABCD, where A indicates nitrile or styrene contents, B the nature of rubber (SBR or NBR); C and D, the nature of filler (either modified, OC or control, N) and its amount (2, 4, 6 or 8). An example is 19 NBR OC 4. In the case of absence of filler, the symbol is kept blank (e.g.: 50NBR).

## 3. Analysis

### 3.1. Transmission electron microscopy (TEM)

The TEM experiments were performed on a HITACHI H-600 at an accelerating voltage of 100 KV. The thin sections required for the TEM experiments were made by cryo-microtoming, at -140°C. The thin sections obtained were about 100 to 200 nm thick.

### 3.2. Atomic force microscopy (AFM)

For tapping mode atomic force microscopy (TMAFM) imaging, specimens were prepared by cryomicrotoming the epoxy coated samples with glass knives at -140°C using liquid nitrogen in a Reichert Jung Ultracut Ultramicrotome. The average thickness of the specimens was 10  $\mu$ m. The measurements of the samples were performed under ambient conditions with a Dimension 3100 and Multimode (JV Scanner) atomic force microscopes, attached to Nanoscope IIIa controller with basic extender (Digital Instruments Inc., USA). The Tapping Mode Etched Silicon Probe (Model

TABLE II Nanocomposites prepared

Sample designation	Compositions	Sample designation	Compositions
23SBROC4	23SBR + OC (4%) + DCP(1%)	34NBROC4	34NBR + OC (4%) + DCP (1%)
23SBRN4	23SBR + N (4%) + DCP (1%)	34NBROC2	34NBR + OC (2%) + DCP (1%)
23SBR	23SBR + DCP (1%)	34NBRN4	34NBR + N (4%) + DCP (1%)
15SBROC4	15SBR + OC (4%) + DCP (1%)	34NBR	34NBR + DCP (1%)
15SBR	15SBR + DCP (1%)	50NBROC4	50NBR + OC (4%) + DCP (1%)
40SBROC4	40SBR + OC (4%) + DCP (1%)	50NBROC8	50NBR + OC (8%) + DCP (1%)
40SBR	40SBR + DCP (1%)	50NBR	50NBR + DCP (1%)
19NBROC4	19NBR + OC (4%) + DCP (1%)	–	–
19NBRN4	19NBR + N (4%) + DCP (1%)	–	–
19NBR	19NBR + DCP (1%)	–	–

LTESP) with resonance frequency of 170 kHz was used. In all the cases, set point ratio was adjusted between 0.7 and 0.8 to avoid tip and sample damage. Height and phase images were recorded simultaneously at the resonance frequency of the cantilever with a scan rate of 1 Hz and a resolution of 256 samples per line. This allowed the resolution of individual primary particle measurements. The images were analyzed using a Nanoscope image processing software.

### 3.3. X-ray diffraction studies

For characterization of the clays and the rubber nanocomposites, X-ray diffraction studies were done using Rigaku CN2005 X-ray Diffractometer “Miniflex” model in the range of  $3^\circ$  to  $10^\circ$  ( $=2\theta$ ). Then,  $d$ -spacing of the clay particles was calculated using the Bragg’s equation.

$$n\lambda = 2d \cdot \sin\theta \quad (1)$$

$\lambda$  = Wavelength of the X-ray (for Cu-target used here, the  $\lambda$  value is  $1.54 \text{ \AA}$ ),  $d$  = interspace distance, and  $\theta$  = angle of incident radiation.

## 4. Results and discussion

### 4.1. Effect of nanoclay on the matrix morphology

#### 4.1.1. SBR matrix

The effect of nanoclay on the morphology has been illustrated by using nanocomposites based on 23SBR rubber with unmodified and modified clays. These are demonstrated in Figs 1a–b and 2a–c. The TEM pictures show that there is a dispersion problem in the case of 23SBRN4 (Fig. 1a). The particles are not exfoliated and there are big lumps in the matrix. On the other hand, the TEM micrographs of 23SBROC4 demonstrate uniform distribution of exfoliated modified clay particles in the matrix (Fig. 1b). The particle size of the clays lies in between 10–15 nm and the aspect ratio is around 100. These data are further confirmed by AFM (Fig. 2a–c). The SBROC4 matrix at two different magnifications clearly shows the exfoliated clay particles uniformly dispersed within the matrix. The average particle thickness lies in the range of 15–20 nm with an aspect ratio of around 100. The pictures also display two different colors of the matrix—probably one for the styrene part and

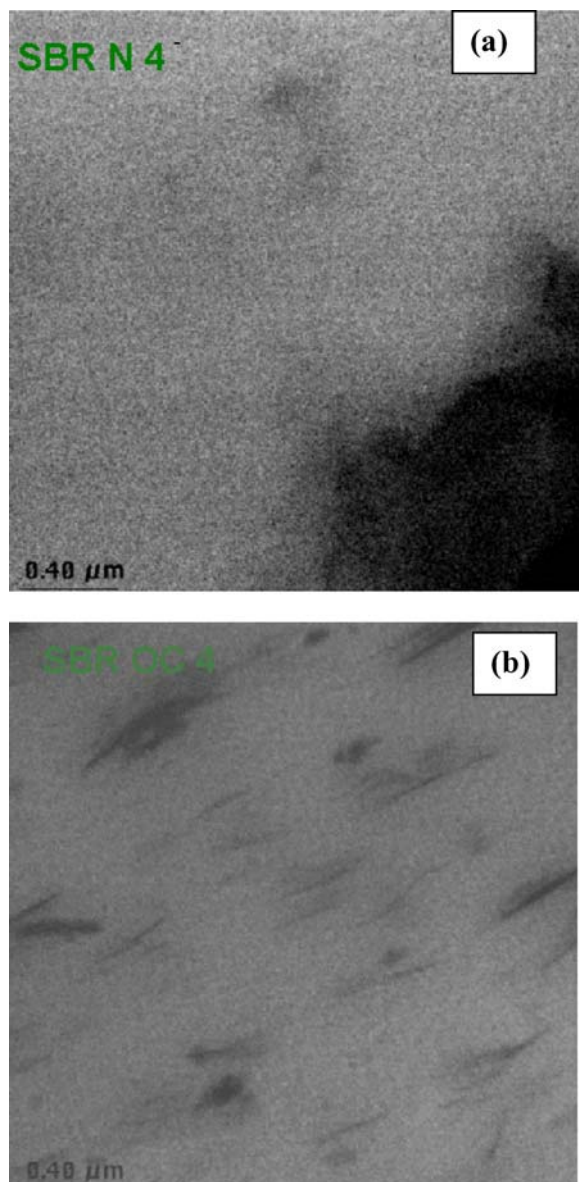
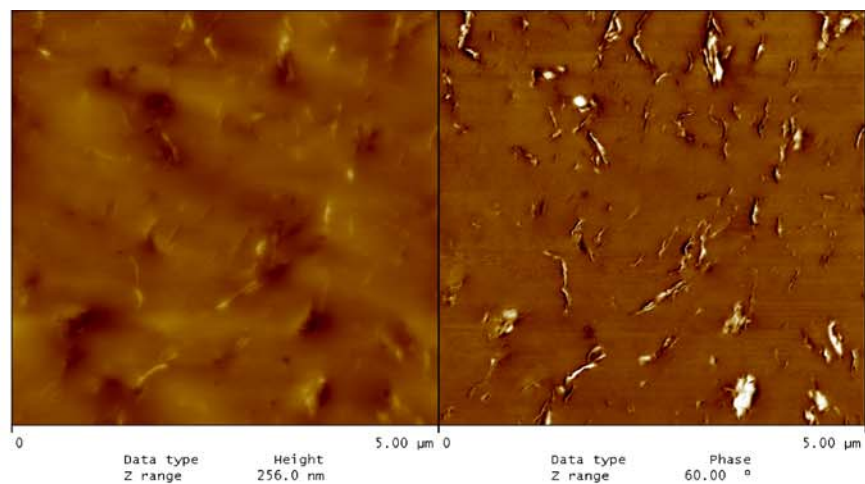


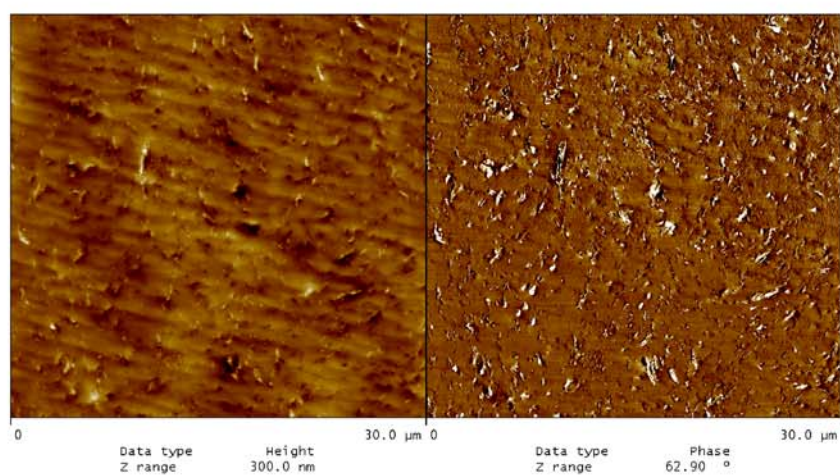
Figure 1 TEM photomicrographs of (a) 23SBRN4 and (b) 23SBROC4.

another for the butadiene part of the SBR co-polymer. The bearing analysis of the SBROC4 is given in Fig. 3, which reveals the distribution of the particles as well as the dimension and parts of the filler in the matrix. It is clear that roughly 5 parts of clay is present on the surface of the matrix i.e., it can be said that the particles are more or less uniformly distributed in the matrix. The bearing area is 5%, while the bearing volume is  $42.48 \mu\text{m}^3$ . On the other hand, the AFM of the SBRN4



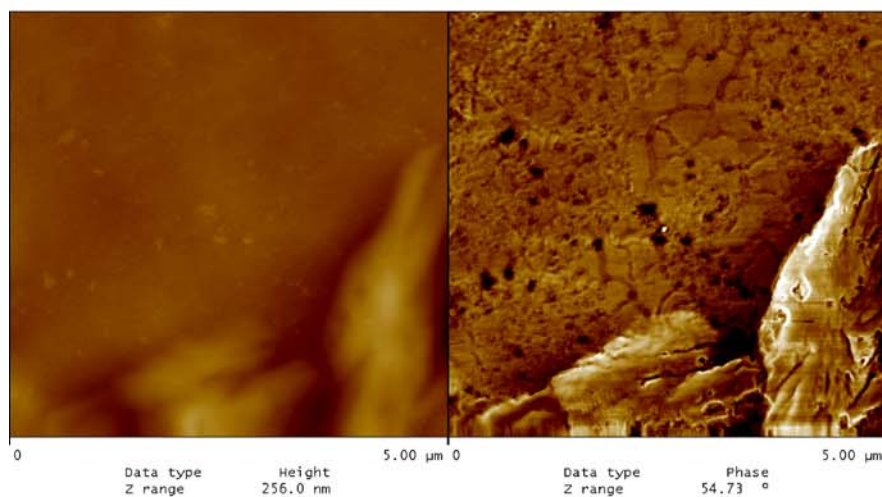
india-sbroc4.003

(a)



india-sbroc4.001

(b)



india-sbrn4.001  
second day after microtoming

(c)

Figure 2 AFM photographs of (a) & (b)23SBROC4 and (c) 23SBRN4.

nanocomposite shows intercalated and agglomerated clay particles, which are not exfoliated. The dimension of the agglomerated particles ranges around 1000 nm. All these observations are supported by the XRD data (Table III), as reported in our earlier communication.

The X-ray diffractogram of 23SBRN4 shows that there is only a small peak around  $4.4^\circ$ , which disappears in 23SBROC4, confirming the absence of layered silicate structure. The values of the gallery distance imply that in the case of the *unmodified* clay SBR composite, the

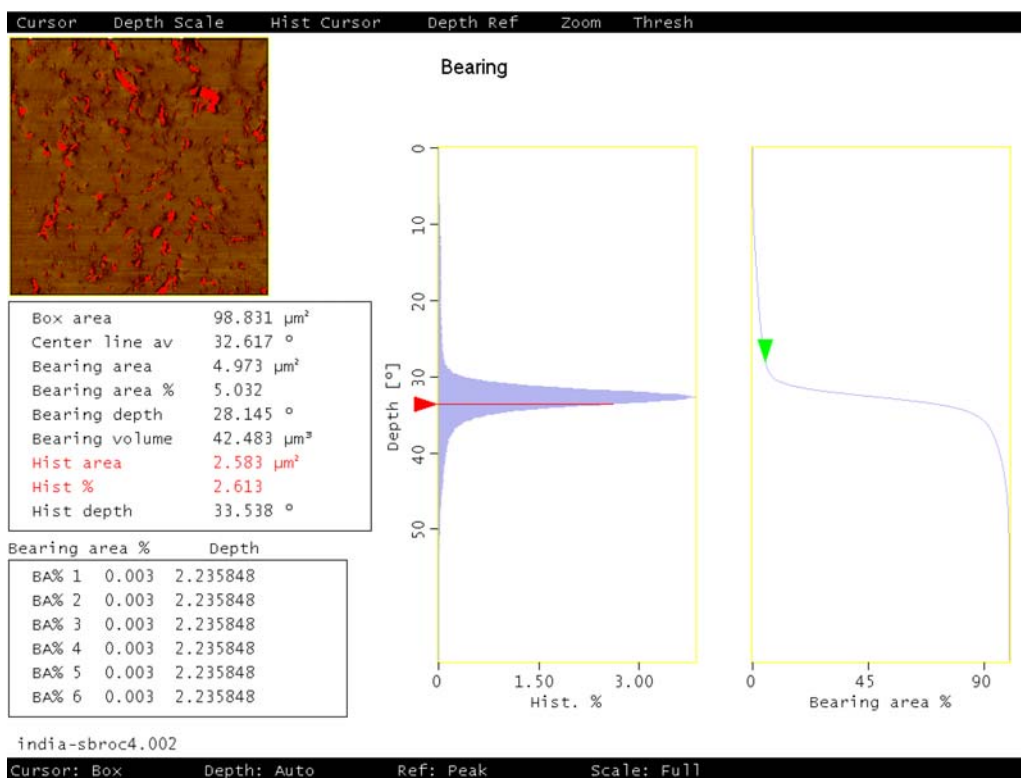


Figure 3 Bearing analysis of the SBROC4.

polymer chains have intercalated into the gallery gap of the clay, although the clays are not exfoliated. The gallery gap in this case is around 20.07 Å.

These results can be explained as follows: The non-polar SBR chains have better interaction with the organically modified nanoclay, compared to the unmodified clay due to better surface compatibility. Hence, the rubber can only remain as intercalated in the gallery gap of N, while it exfoliates the OC layers. Some van der Waals type of interaction between the long carbon chains of the clay modifier and the nonpolar polymer chains is responsible for this reason.

**4.1.1.1. Effect of styrene content in SBR.** Three different grades of SBR with 15, 23 and 40% styrene content were used to prepare the nanocomposites. The morphology has been studied using TEM and XRD. From

TABLE III X-ray results\*

Samples	Peak position ( $2\theta$ )	Gallery gap (Å)
N	7.5	11.61
OC	4.9	18.01
15SBRN4	NO PEAK	–
15SBROC4	NO PEAK	–
23SBRN4	4.4	20.07
23SBROC4	NO PEAK	–
40SBRN4	NO PEAK	–
40SBROC4	NO PEAK	–
19NBROC4	4.2	21.09
34NBRN4	7.2	12.26
34NBROC2	7.2	12.27
34NBROC4	6.9	12.80
50NBROC4	5.4	16.40
50NBROC8	7.2	12.27

\*Taken from reference 16; 1 nm = 10 Å.

the TEM (Figs 1 and 4) photomicrographs, it can be seen that the clay particles are totally exfoliated and the average particle thickness are in the range of 10–15 nm in every case. The XRD results (Table III) indicate that in all the SBROC4s the clay particles are exfoliated leading to absence of any peak. The TEM and XRD data display a similar kind of morphology in the three different SBR systems. In all the cases, the organically modified clay can easily mix with the nonpolar rubber, which can intercalate into the gallery very easily to exfoliate the clay layers.

**4.1.1.2. Effect of solvent on morphology of nanocomposites.** The effect of solvent used to prepare the nanocomposites has been studied using 23SBROC4 which has been prepared in two different solvents namely: toluene and chloroform. In toluene, the particles are totally exfoliated, whereas in chloroform the particles are mostly exfoliated (Fig. 5). The average thickness of the particles are 10–20 nm in both the cases, although there are few thick particles present in chloroform based sample.

#### 4.1.2. 34NBR matrix

TEM photomicrographs (Fig. 6) show that the clays are not distributed uniformly in 34NBRN4 matrix. Some of the unmodified clays are agglomerated and remain unexfoliated in the matrix. The average particle dimensions including smaller and larger particles are 100 to 150 nm. On the other hand, 34NBROC4 shows particles having layered structures intact, without any agglomeration. The particle dimension lies between 50 to 70 nm due to intercalation of the polymer chains inside the gallery gap of the nanoclay (which has dimension

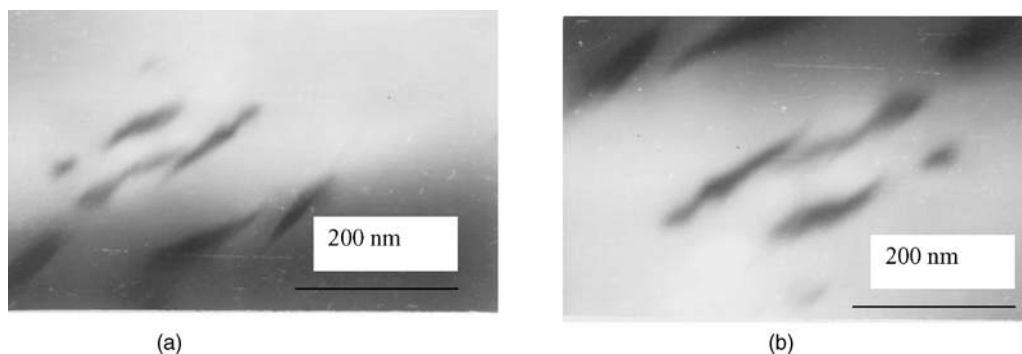


Figure 4 TEM photos of (a) 15SBROC4 and (b) 40SBROC4.

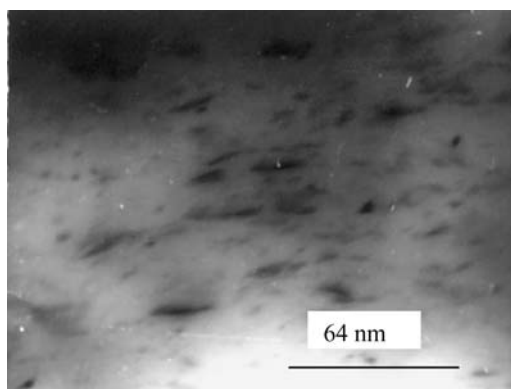


Figure 5 TEM photographs of 23SBROC4 in chloroform.

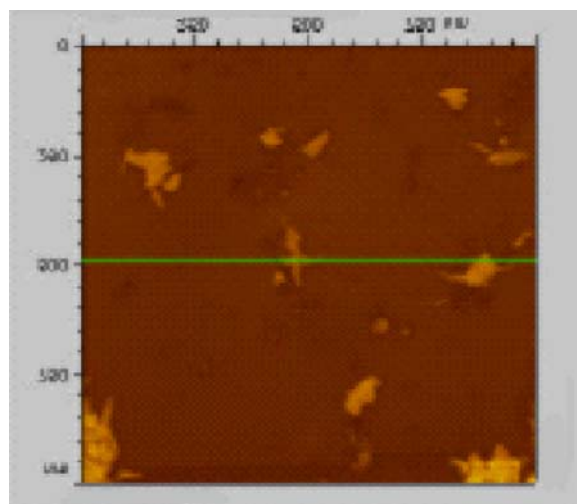


Figure 7 AFM photos of 34NBROC4.

initially 50 nm). Due to intercalation, the gap between the two layers has increased, but since they are not totally exfoliated, the whole layered structure appears as one thick sheet. The AFM of the 34NBROC4 is given in Fig. 7, which again confirms the intercalation rather than exfoliation of the particles. The particles are uniformly distributed in the matrix and the thickness lies around 50 nm. The percentage of the particles present is also around 4% signifying uniform distribution of the particles.

34NBRN4 shows a peak at  $7.2^\circ$ , while 34NBROC4 gives a peak at  $6.9^\circ$  (Table III). In both the cases, it is clearly evident that the clay layers are not exfoliated. In the case of 34NBROC4, the polymer chains have intercalated into the gallery gap to some extent and results in an increase in gallery gap from  $12.26 \text{ \AA}$  up to  $12.80 \text{ \AA}$  when compared with the 34NBRN4.

This can be explained as follows: Few OH groups are present on the surface of the clay, which are possibly

capable of forming H-bonds with the CN groups of the polymer chains. Hence, the polymers only form H-bonds with the surface OH groups of the clay, but does not intercalate. OC is organically modified clay. 34NBR being a polar rubber is incompatible with the organic surface of the clay. Only in the case of OC, a little intercalation is showed by 34NBR probably due to the interaction between the butadiene part of the NBR and the organic surface of the clay.

4.1.2.1. *The effect of nitrile content in NBR on morphology.* The effect of nitrile content on the morphology of the polar rubber nanocomposite has been studied using 19NBR, 34NBR and 50NBR. The TEM pictures

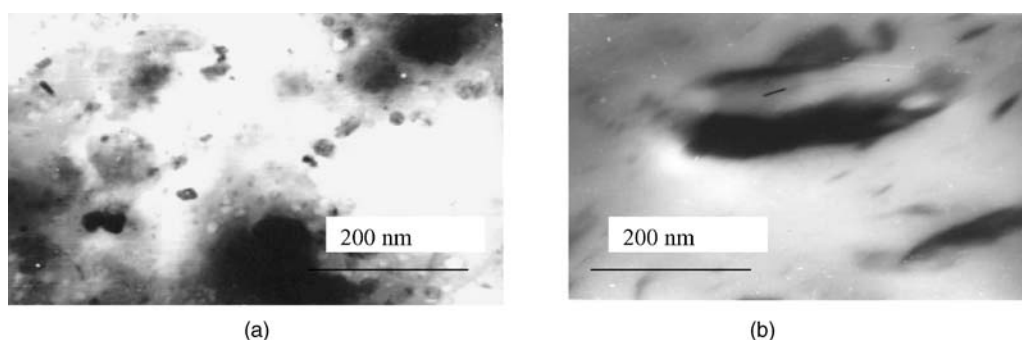


Figure 6 TEM photographs of (a) 34NBRN4 and (b) 34NBROC4.

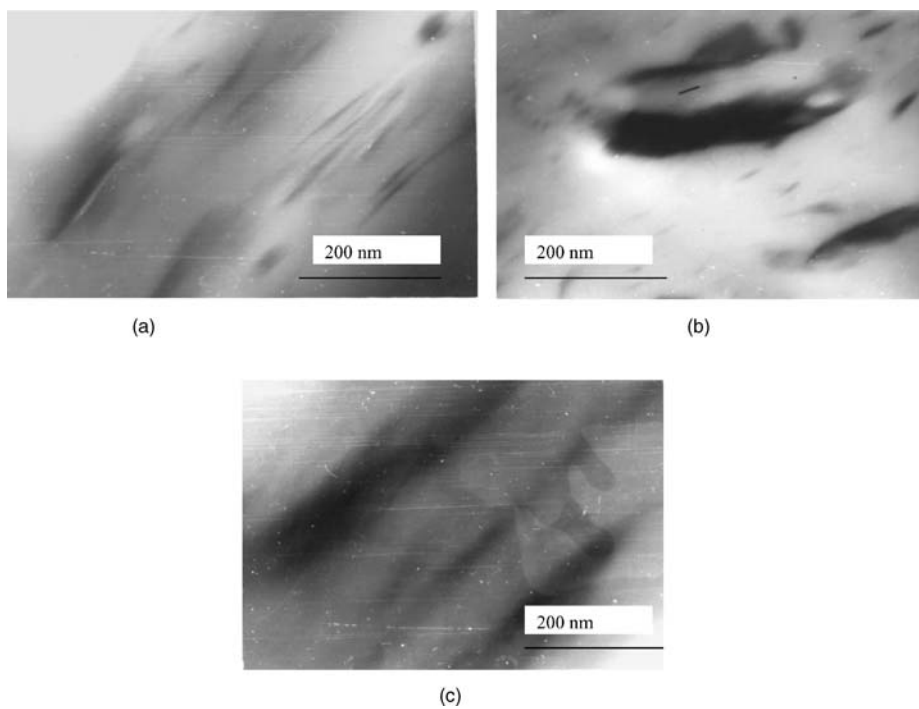


Figure 8 TEM photos of (a) 19NBROC4, (b) 34NBROC4 and (c) 50NBROC4.

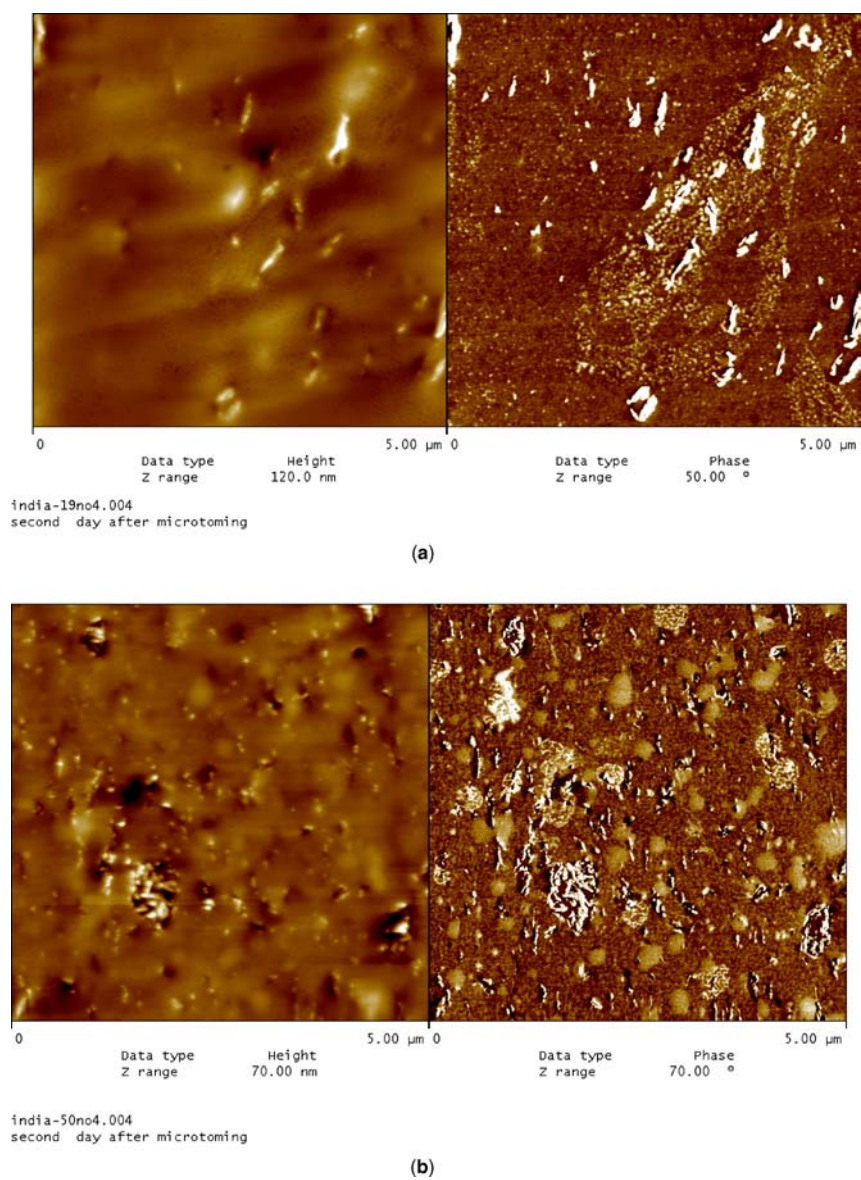


Figure 9 AFM photos of (a) 19NBROC4 and (b) 50NBROC4.

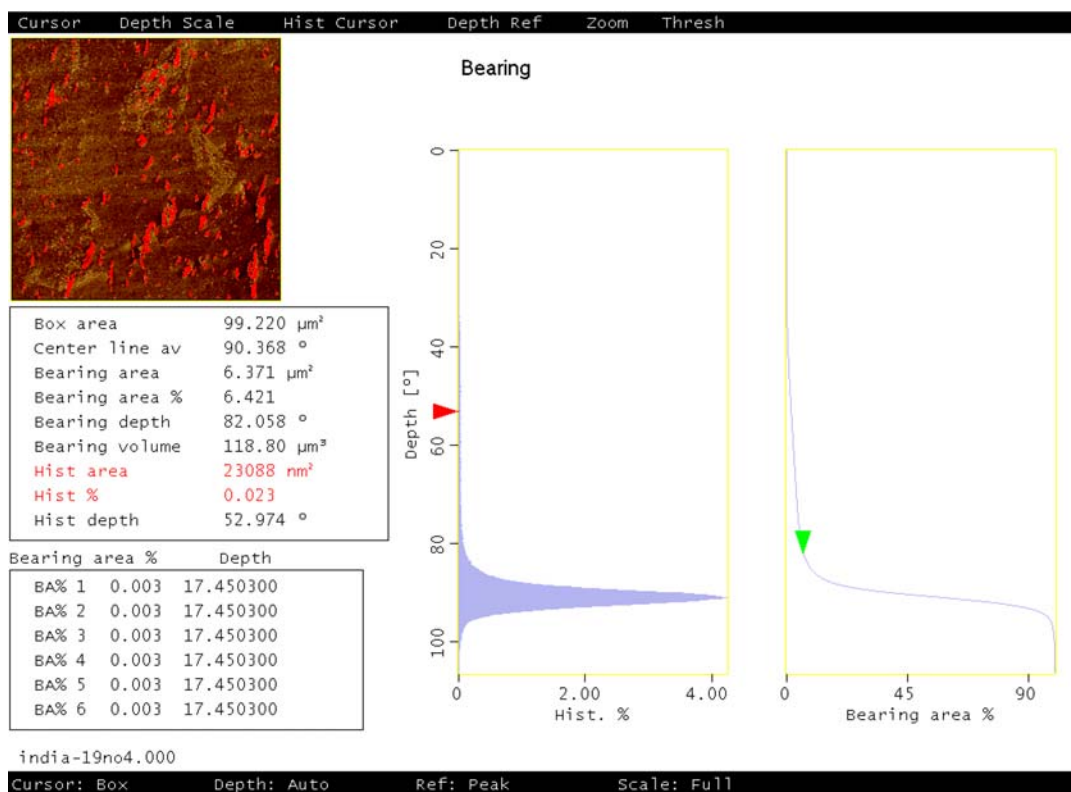


Figure 10 Bearing analysis of 19NBROC4.

of the modified clay composites of 19NBR, 34NBR and 50NBR are given in Fig. 8a–c. The micrograph of 19NBROC4 (Fig. 8a) shows particles, which are predominantly exfoliated along with a few unexfoliated thick particles. The average thickness of these particles is 15 to 20 nm and the aspect ratio is near about 90–100. But the micrographs in the case of 34NBROC4 and 50NBROC4 show clearly that the particles are thick and layered. They are not exfoliated, but only intercalated. The average thickness of these particles fall in the range of 50–70 nm and 70–100 nm for 34NBROC4 and 50NBROC4 respectively. The unmodified clay nanocomposite of both 34NBR and 50NBR at 4% loading are unexfoliated. AFM of the three NBR-OC4 composites has been done. The micrographs of 19NBROC4, 50NBROC4 and 34NBROC4 are given in Figs 7 and 9a–b. The particle dimension in 19NBR matrix is around 20–25 nm, whereas the particles are much bigger in the case of 34NBR and 50NBR. The average thickness of the particle remains in the range of 70–100 nm for 50NBROC4 and 50–70 nm in the case of 34NBROC4. In the later two cases the particles are agglomerated which has been depicted also in the TEM photographs. It is interesting to note that the surface of 50NBROC4 shows three textures—one for the filler and the remaining two for the constituents (acrylonitrile and butadiene) of the copolymer. It is also noteworthy that the clays are uniformly distributed and the average particle concentration is 5–6% as shown by the bearing analysis (Fig. 10). The XRD study indicates that the OC composites of 50NBR and 34NBR give prominent peaks at  $5.4^\circ$  and  $6.9^\circ$  respectively, whereas 19NBROC4 gives a peak at  $4.2^\circ$ , which corresponds to a  $d$ -value of

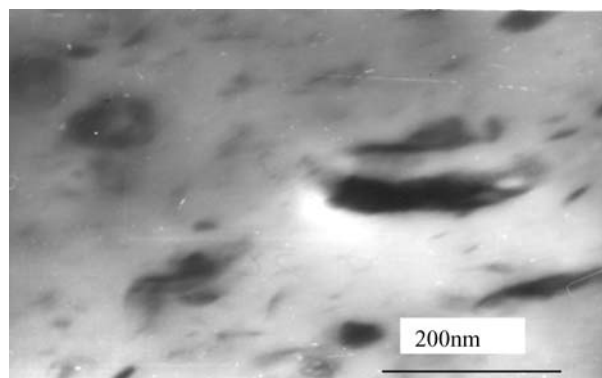


Figure 11 TEM photo of 34NBROC2.

21.09 Å. The modified clay having a better interaction with the nonpolar rubber, gives a highly intercalated nanocomposites with 19NBR but with increasing polarity (34NBR and 50NBR) the extent of intercalation is low. In the later two cases the high acrylonitrile content of the NBRs makes the polymers incompatible with the modified clay. NBRs have CN groups, which can make H bonds with the surface OH groups of the clay. The extent of H bond formation depends on the CN content. After satisfying all the OHs on the surface, the polymer chains can intercalate a little inside the gallery due to nonpolar-nonpolar interaction between the butadiene part and the clay surface modifier. That is why slight intercalation is possible in 34 and 50% NBROC4s. In 19NBR the nitrile content is very low, so the H bond formation will be very low. Due to extensive intercalation, partial exfoliation has occurred [16].



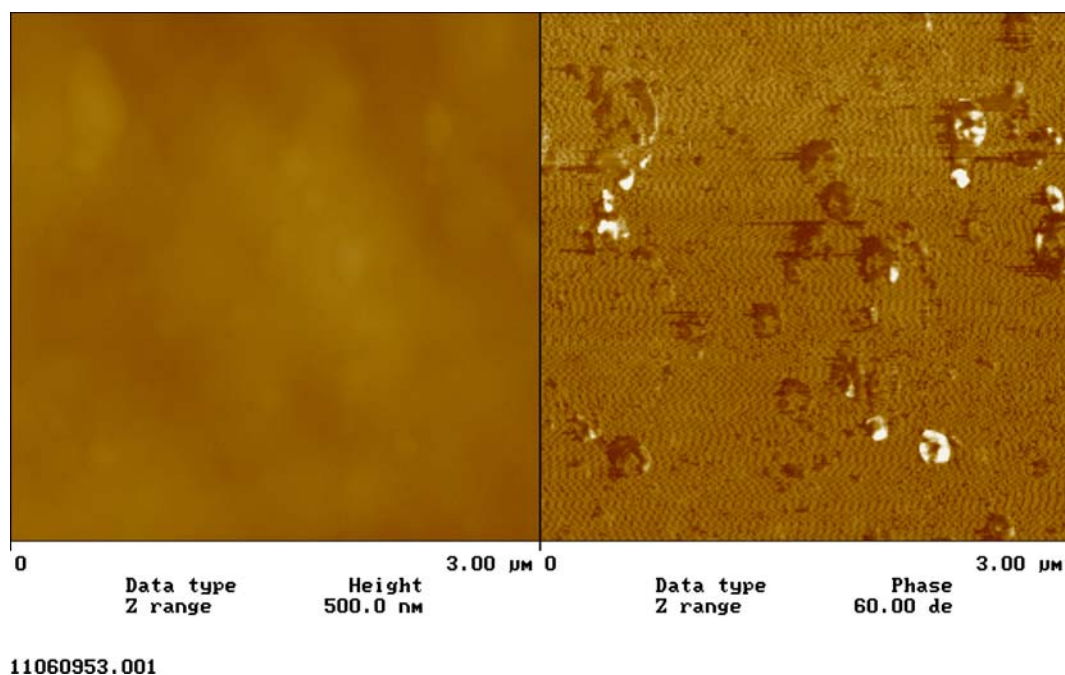


Figure 12 AFM photos of 50NBROC8.

#### 4.1.3. Effect of filler loading on morphology of the matrix

To study the effect of filler loading on the morphology of the nanocomposites, modified clay (OC) at two different loadings (2 and 4 phr for 34NBR and 4 and 8 phr for 50NBR) has been used. TEM photographs of 2 and 4 phr loaded samples are shown in Figs 11 and 6b respectively. The average thickness of the layered particles in 2 phr loaded sample is 30 nm, while the same for the 4 phr loading is 50–70 nm. In each case, most of the particles are not exfoliated, but intercalated and remain as layered structure. The extent of intercalation in 4 phr loading is more. The XRD (Table III) study also reveals that there is no exfoliation in either of the cases, but the peak height increases with higher filler loading [16].

For 50NBR system also, the clays in neither 4 phr nor 8 phr OC loaded systems are exfoliated. AFM of these two systems (Figs 9b and 12) show similar morphology, particle dimensions and the particle distribution. The XRD data also confirm the same [16].

When fillers are added to the NBR matrix the polymer chains try to intercalate into the gallery gap. At certain filler loading (4 phr) the extent of intercalation reaches an optimum. Beyond that the fillers start getting agglomerated and thus the XRD peak intensity increases and the peak position shifts towards right. Hence 4 phr loaded sample shows thicker clay particles compared to that of the 2 phr loaded composite.

## 5. Conclusions

Nanocomposites were prepared using unmodified and modified clay and three different grades each of SBR having 15, 23 and 40% styrene contents, and of NBR having 19, 34 and 50% acrylonitrile contents. The following observations have been made:

(1) The unmodified clay filled 23SBR nanocomposite shows unexfoliation, agglomeration and big lumps of clay, whereas the modified clay filled nanocomposite demonstrate exfoliation over the whole matrix. These particles in the later case have a dimension in the range of 10–15 nm as confirmed by both AFM and TEM.

(2) The three grades of SBR gives completely exfoliated clay structure when OC is added to the rubber. TEM micrographs have shown that all three SBRs give similar morphology, independent of styrene content of the rubber.

(3) The TEM micrographs of the SBROC4 composites prepared in toluene and chloroform provide the same information, although the composite prepared in chloroform contains few thicker particles.

(4) 34NBR being a polar rubber is not compatible with N and the organically modified OC. But N remains as agglomerated particles and clusters, while OC shows better dispersion although it is not exfoliated. The particle dimension of the clays in 34NBROC4 ranges in between 50–70 nm.

(5) The acrylonitrile content of the NBR influences the morphology of the nanocomposites. 50NBR and 34NBR do not exfoliate the clay and have particles ranging from 50–70 nm thick and 70–100 nm thick respectively. But 19NBR having a very low polarity can intercalate to a great extent and gives mostly exfoliated particles having a dimension of 10–20 nm.

(6) Loading of filler beyond an optimum value causes agglomeration, shown by AFM and TEM photographs.

## Acknowledgement

We are grateful to (1) Dr. Bede Pittenger and Natalia Erina, Veeco Metrology Group, Digital Instruments, California, U.S.A. for taking the AFM photographs and (2) DRDO, New Delhi for sponsoring the project.

## References

1. B. K. G. THENG, "Formation and Properties of Clay-Polymer Complexes" (Amsterdam, Elsevier, 1979) p. 133.
2. A. OKADA, M. KAWASUMI, A. USUKI, Y. KOJIMA, T. KURAUCHI and O. KAMIGAITO, *Mater Res. Soc. Proc.* **171** (1990) 45.
3. T. J. PINNAVAIA, T. LAN, Z. WANG, H. SHI and P. D. KAVIRATNA, *ACS Symp Ser.* **622** (1996) 250.
4. P. B. MESSERSMITH and E. P. GIANNELLIS, *Chem Mater.* **6** (1994) 1719.
5. P. KELLY, A. AKELEH, S. QUTUBUDDIN and A. MOET, *J. Mater. Sci.* **29**(9) (1994) 2274.
6. X. KOMMANNAN, L. A. BERGLUND, J. STERTE and E. P. GIANNELLIS, *Polym. Engng. Sci.* **38** (1998) 1351.
7. P. B. MESSERSMITH and E. P. GIANNELLIS, *Chem Mater.* **5** (1993) 1064.
8. *Idem.*, *J. Polym. Sci.: Polym. Chem.* **33** (1995) 1047.
9. S. BURNSIDE and E. P. GIANNELLIS, *Chem. Mater.* **7** (1995) 1597.
10. S. WANG, C. LONG, X. WANG, Q. LI and Z. QI, *J. Appl. Polym. Sci.* **69** (1998) 1557.
11. R. A. VAIA, H. ISHII and E. P. GIANNELLIS, *Chem. Mater.* **5** (1993) 1694.
12. K. YANO, A. USUKI, A. OKADA, T. KURAUCHI and O. KAMIGAITO, *J. Polym. Sci.: Polym. Chem.* **31** (1993) 2493.
13. N. HASEGAWA, M. KAWASUMI, M. KATO, A. USUKI and A. OKADA, *J. Polym. Sci.* **63** (1997) 137.
14. Y. KE, C. LONG and Z. QI, *J. Appl. Polym. Sci.* **1** (1997) 1139.
15. Z. WANG and T. PINNAVAIA, *J. Chem. Mater.* **10** (1998) 3769.
16. S. SADHU and A. K. BHOWMICK, *J. Polym. Phys.: Part B* **42** (2004) 1573.
17. S. N. MAGANOV, V. ELLINGS and M. H. WHANGBO, *Surf. Sci.* **375** (1997) L385.
18. M. COSTER and J. L. CHERMANT, *Precis d'analyse d'image*: Presses du CNRS (1989).
19. S. RAY, A.K. BHOWMICK and S. BANDYOPADHYAY, *Rubber Chem. Technol.* **76** (2003) 1091.
20. A. M. SHANMUGHARAJ, S. RAY, S. BANDYOPADHYAY and A. K. BHOWMICK, *J. Adhesion Sci. Technol.* **17** (2003) 1167.

*Received 28 January  
and accepted 9 September 2004*